HHS Public Access

Author manuscript

Behav Brain Res. Author manuscript; available in PMC 2020 December 16.

Published in final edited form as:

Behav Brain Res. 2019 December 16; 375: 112116. doi:10.1016/j.bbr.2019.112116.

Cerebral Perfusion Mapping During Retrieval of Spatial Memory in Rats

DP Holschneider[a,b,c,*], **TK Givrad**[c,1], **J Yang**[a], **SB Stewart**[a,2], **SR Francis**[a], **Z Wang**[a], **JMI Maarek**[c]

[a]Depts. of Psychiatry and the Behavioral Sciences, Keck School of Medicine, Los Angeles, CA, 90033

[b]Dept. of Neurology, Keck School of Medicine, Los Angeles, CA, 90033

[c]Dept. of Biomedical Engineering, Viterbi School of Engineering, University of Southern California, Los Angeles, CA, 90089

Abstract

Studies of brain functional activation during spatial navigation using electrophysiology and immediate-early gene responses have typically targeted a limited number of brain regions. Our study provides the first whole brain analysis of cerebral activation during retrieval of spatial memory in the freely-moving rat. Rats (LEARNERS) were trained in the Barnes maze, an allocentric spatial navigation task, while CONTROLS received passive exposure. After 19 days, functional brain mapping was performed during recall by bolus intravenous injection of [^{14}C]-iodoantipyrine using a novel subcutaneous minipump triggered by remote activation. Regional cerebral blood flow (rCBF)-related tissue radioactivity was analyzed by statistical parametric mapping from autoradiographic images of the three-dimensionally reconstructed brains. Functional connectivity was examined between regions of the spatial navigation circuit through interregional correlation analysis.

Significant rCBF increases were noted in LEARNERS compared to CONTROLS broadly across the spatial navigation circuit, including the hippocampus (anterior dorsal CA1, posterior ventral CA1–3), subiculum, thalamus, striatum, medial septum, cerebral cortex, with decreases noted in the mammillary nucleus, amygdala and insula. LEARNERS showed a significantly greater positive correlation of rCBF of the ventral hippocampus with retrosplenial, lateral orbital, parietal and primary visual cortex, and a significantly more negative correlation with the mammillary nucleus, amygdala, posterior entorhinal cortex, and anterior thalamic nucleus. The complex sensory component of the spatial navigation task was underscored by broad activation across

[*]**Corresponding author:** Daniel P. Holschneider, MD, University of Southern California, 1975 Zonal Ave., KAM 400, MC 9037, Los Angeles, CA 90089-9037, Tel: (323)442-1536, Fax: (323)442-1587, holschne@usc.edu.

[1]Present address: Dept. of Mathematics, California State University, Los Angeles, CA, USA

[2]Present address: Dept. of Family Medicine, University of Colorado School of Medicine, Denver, Co, USA

Conflict of interest

The authors declare that they have no conflict of interest

visual, somatosensory, olfactory, auditory and vestibular circuits which was enhanced in LEARNERS. Brain mapping facilitated by an implantable minipump represents a powerful tool for evaluation of mammalian behaviors dependent on locomotion.

GRAPHICAL ABSTRACT

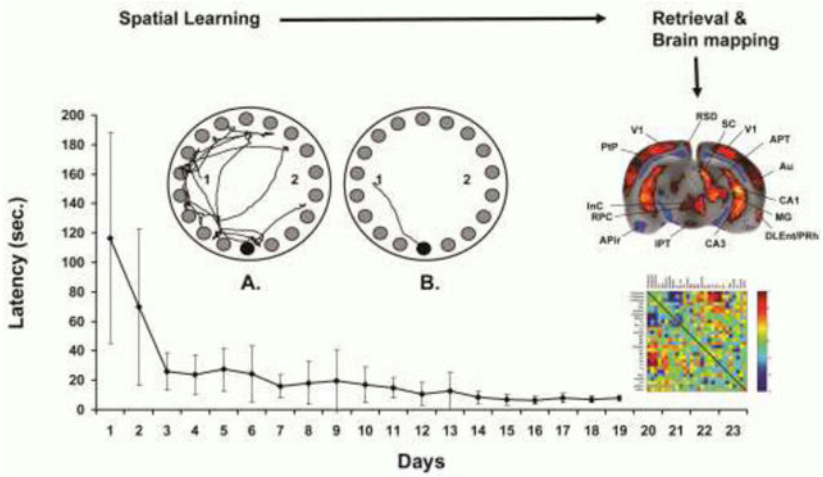

Keywords

spatial memory; hippocampus; allocentric; functional neuroimaging; brain mapping; implantable device

1. Introduction

The Barnes maze, a hippocampus-dependent spatial memory task, is widely used for cognitive testing in rodents [1]. To our best knowledge, functional brain activation during Barnes maze retrieval has not been studied at the whole-brain level, and how multiple brain regions interact with the hippocampus and with each other remains to be investigated. Despite continuing debate about the precise relationship between neural firing, regional cerebral blood flow (CBF) and metabolism, as well as the role of vascular distribution and architecture in health and disease [2, 3], the existence of cerebral perfusion coupling to neural activity is well accepted in normal subjects and forms the basis of the majority of functional brain mapping studies. We have in the past developed a self-contained, implantable minipump that allows intravenous bolus administration of cerebral perfusion tracers by remote activation, and thereby allows the functional brain mapping of complex behaviors in freely moving animals.[4, 5] We now demonstrate the application of this novel minipump for the functional brain mapping of spatial memory retrieval using the Barnes maze. In the current study, we use our minipump to administer a cerebral perfusion tracer as an intravenous bolus during performance of the previously learned navigation task, followed immediately by lethal injection, rapid removal of the brain, and analysis of regional cerebral blood flow tissue radioactivity with the use of autoradiography.

The current study is the first to report functional maps of the whole brain during Barnes maze performance in the nontethered, awake animal with a temporal resolution of 5–10 seconds [4] and a spatial resolution of ~100 μm. [6] Furthermore, correlation-based functional connectivity analysis is applied to assess functional interaction among brain regions showing task-specific activation [7].

2. Materials and methods

2.1. Animals

Experiments were conducted under a protocol approved by the Institutional Animal Care and Use Committee of the University of Southern California, an institution approved by the Association for Assessment and Accreditation of Laboratory Animal Care, and in compliance with the National Institutes of Health guide for the care and use of Laboratory animals. Male Sprague Dawley rats (350 ± 23 g) were singly housed in the vivarium on a 12-hour light cycle (lights out 7 p.m. to 7 a.m.) and received standard rodent chow and water ad lib. Behavioral training began 10 days after delivery of the animals to the vivarium from the vendor (Envigo, Placentia, CA, USA). All efforts were made to minimize animal suffering.

2.2. Barnes maze

2.2.1 Apparatus: The black-surface Barnes maze (diameter 122 cm, height 94 cm) with 18 holes (diameter 10.8 cm) spaced in 20 degree intervals around the periphery was illuminated by ceiling fluorescent bulbs in a quiet room (62 dB sound level).[1] A ‘safe’-box made of black plastic (42 cm × 17 cm × 13 cm, length × width × height) was mounted under one of the 18 holes of the maze, with the other holes remaining open. To avoid reflections from the floor offering differing visual cues between the open holes and the safe-box, a black cloth ‘skirt’ that descended to the ground was fixed to the rim of the maze. A cylindrical start box (diameter 17 cm diameter, height 17 cm) was used to release the animal into the maze. Spatial cues on the walls of the room remained fixed and could be used by the animal as reference points for spatial navigation.

2.2.2. Barnes maze training: Animals were transferred from the vivarium to a separate room of the laboratory 1 hour prior to testing and returned to the vivarium 1 hour following the final trial. A trial began with placement of the rat facing a random direction in the cylindrical start box whose position was altered in a pseudorandom fashion for each trial between two starting positions (see Fig. 1). This randomization of the start position allowed for navigation that was dominantly mediated by external (allocentric), rather than internal (egocentric) cues to the animal. Rats remained in the start box for 30 seconds, during which time a white-noise generator (80 dB) hung from the ceiling above the maze was turned on. Rats were released into the maze when the start box was pulled vertically upwards by a manual pulley system activated from outside the experimental room. The maximum trial duration to find the safe-box was 4 minutes. Typically, the latency to find the safe-box dropped below 30 seconds by day 3 of training (Fig. 1). Once inside the safe-box, the white noise generator was turned off and the rat was left undisturbed for 60 seconds. If an animal failed to find the safe-box in 4 minutes, it was manually placed into the box and left there for

60 seconds. To minimize odor cues between trials, fecal pellets were removed, the maze and safe-box were wiped down with a 1% solution of ammonia, rinsed with water, then dried, and the surface of the maze was rotated (0°, 90°, 180°, or 270° in pseudorandom sequence) with respect to the safe-box, which remained in a fixed position. Animals (n = 11) were trained starting at 9 a.m. for 19 consecutive days (3 trials/day with 10 min. intertrial intervals). Control animals (n = 8) received identical handling, except that they were exposed daily to the maze only for 30 seconds without the presence of the 'safe-box.' The animal's path in the maze was tracked by a video camera mounted above the maze and recorded on video tape. The rat's progress in the maze was monitored on a video monitor in an adjacent room, such that the experimenter was not in the room during the animal's trial.

2.3. Surgical implantation of the microbolus infusion pump (MIP)

Following the training, a minipump was implanted subcutaneously on the rat's dorsum under isoflurane anesthesia (1.2%), with placement of the outflow catheter into the external jugular vein.[4] A percutaneous port allowed for postoperative flushes of the catheter and for loading of the radiotracer 40 minutes prior to imaging. After MIP implantation, rats were returned to their home cages for recovery for 3 days without further training. Postoperatively, catheters were flushed every 2 days with 0.8 ml of 5 U/ml heparin (0.9% normal saline). The MIP, as previously described [4, 5], consists of (a) an intravenous silastic catheter (5Fr) connected to (b) a silicone-embedded solenoid valve powered by a lithium battery rechargeable by wireless power transfer and gated by a frequency-sensitive (30 kHz) photodetector, (c) an ejection chamber containing the radiotracer, and (d) a silastic reservoir containing a euthanasia solution (Fig. 1). The photodetector with peak optical sensitivity in the near-infrared spectrum allowed for transcutaneous triggering of the pump with trains of light pulses from five external near-infrared light emitting diodes (LEDs, Lumex Opto, Carol Stream, IL, USA), individually mounted on the four walls and ceiling of the experimental room and remotely controlled.

2.4. Brain mapping

On postoperative day 4 (post-acquisition delay), the animal was restrained for 3 minutes to allow for loading of the MIP through the percutaneous port with the cerebral blood flow (CBF) tracer [^{14}C]-iodoantipyrine (100 μCi/kg in 300 μl of 0.9% saline, American Radiolabeled Chemicals, MO, USA). Thereafter, the euthanasia solution (1.0 ml of pentobarbital 75 mg/kg, 3 mol/l KCl) was loaded into the reservoir. After removal from the restraining device (Decapicone, Braintree, MA), rats were allowed to recover undisturbed in a quiet environment for 40 minutes. Prior to imaging, rats were reexposed to the Barnes maze paradigm in a single 20-second trial, and then returned to a metal shoe box cage. Ten minutes later, during the imaging paradigm, the rat was re-exposed one more time to the Barnes maze in which the safe-box had been removed. Given the choice to remove or retain the safe-box on the day of imaging, we chose to remove it. This allowed continuation of the search strategy of the animal, rather than of arrival within the safe-box which might have elicited a 'reward' response on completion of the task. The MIP was triggered transcutaneously by activating the ceiling and wall LEDs in the experimental room. Activation of the LEDs was initiated manually outside this room by the experimenter at a time displayed on a video monitor, when the rat was within a body's length of the hole that

previously provided entry to the safe-box (LEARNERS). CONTROLS following release into the maze would also actively explore though in a non-directed fashion. Triggering times in the CONTROLS were matched to those in the LEARNERS. Triggering the MIP resulted in intravenous bolus release of the pump's radiotracer into the animal's circulation, followed immediately by injection of the euthanasia solution. This resulted in cardiac arrest within ~5–10 seconds from the time of injection, a precipitous fall of arterial blood pressure, termination of brain perfusion, and death.[4] This 5–10 seconds period constituted the temporal resolution of resulting perfusion maps.

Brains were rapidly removed, flash-frozen, and cryosectioned (fifty-eight 20 μm coronal slices starting 3.9 mm anterior to bregma with a 300 μm interslice distance). Sections were heat-dried on glass slides and exposed for 2 weeks to Ektascan Diagnostic Film (Eastman Kodak, Rochester, NY, USA) in spring-loaded x-ray cassettes along with 16 radioactive ^{14}C standards (Amersham Biosciences, Piscataway, NJ, USA). Autoradiographs were placed on a voltage stabilized light box with diffuser plate (Northern Lights Illuminator, InterFocus Ltd, England), imaged with a Retiga 4000R charge-coupled device monochrome camera (Qimaging, Surrey, BC, Canada), and digitized on an 8-bit gray scale using Qcapture Pro 5.1 (Qimaging) on a personal computer.

Regional cerebral blood flow (rCBF)-related tissue radioactivity was measured by the classic [^{14}C]-iodoantipyrine method.[8–10] In this method, there is a strict linear proportionality between tissue radioactivity and CBF when the data is captured within a brief interval (~10 seconds) after the tracer injection.[11, 12] Perfusion mapping using autoradiographic methods [13] fills a gap in the current armamentarium of imaging tools in that it can deliver a three-dimensional assessment of functional activation of the awake, nonrestrained animal, with a temporal resolution of ~5–10 seconds [4] and spatial resolution of 100 μm.[6]

2.5. Data analysis

2.5.1 Behavior: Latency to reach the 'safe box' was recorded by stopwatch from the video recordings in a blinded fashion. Latencies were averaged across the 3 daily trials for each animal and group averages were calculated. For the brain mapping trials, a single latency was recorded for each animal. In addition, a visual grid of 4.6 cm^2 squares was superimposed on the recorded video images of the Barnes Maze, and the number of boxes traversed by each animal was recorded during the imaging trials. Group averages (± standard deviations) were calculated.

2.5.2. Statistical parametric mapping: rCBF was quantified by autoradiography and analyzed on a whole-brain basis using statistical parametric mapping (SPM, version SPM8, Wellcome Centre for Neuroimaging, University College London, London, UK). SPM, a software package developed for analysis of imaging data in humans [14] has been adapted by us [13] for use in autoradiographs of the rat brain. A three-dimensional reconstruction of each animal's brain was conducted using 58 serial coronal sections (voxel size: 42 μm × 42 μm × 300 μm). Adjacent sections were aligned both manually and using TurboReg, an automated pixel-based registration algorithm.[15] After three-dimensional reconstruction, one "artifact free" brain was selected as reference and smoothed with a Gaussian kernel

(FWHM = 3 × voxel dimension). Brains from both groups were spatially normalized to the smoothed reference brain. Following spatial normalization, normalized images were averaged to create a mean image, which was then smoothed to create the final brain template. Each original three-dimensional reconstructed brain was then spatially normalized into the standard space defined by the template. An unbiased, voxel-by-voxel analysis of whole-brain activation using SPM was used for detection of significant group differences in functional brain activation. To ensure that only voxels mapping cerebral tissue were included in the analysis, voxels for each brain failing to reach a specified threshold (70% of the mean voxel value) were masked out to eliminate the background and ventricular spaces without masking gray or white matter. Global differences in the absolute amount of radiotracer delivered to the brain were adjusted in SPM for each animal by scaling the voxel intensities so that the mean intensity for each brain was the same (proportional scaling). Significance ($P<0.05$) was established at the voxel and cluster level (minimum cluster extent of 100 contiguous voxels). In addition, we examined the false discovery rate ($P < 0.05$), which controls the expected proportion of false positives among suprathreshold voxels [16]. Brain regions were identified using coronal, sagittal and transverse views from a rat brain atlas [17], as well as the hippocampal parcellation scheme of Kjonigsen et al.[18] Postrhinal cortex was defined using the definition of Burwell (2001).[19]

2.5.3. Interregional correlation analysis: We applied interregional correlation analysis to investigate functional connectivity as previously described.[7] This is a well-established method, which has been applied to analyze rodent brain mapping data of multiple modalities, including autoradiographic deoxyglucose uptake [20–22], autoradiographic CBF [23], cytochrome oxydase histochemistry [24–26], and fMRI.[27] In these studies, correlations are calculated in an intersubject manner, i.e., across subjects within a group. This differs from the intra-subject cross correlation analysis often used on fMRI time series data.[28]

ROIs examined were regions of the spatial navigation circuit, including the hippocampal formation (ventral CA1, CA2, CA3, dentate gyrus, subiculum), cerebral cortex (anterior cingulate, auditory, anterior entorhinal, posterior entorhinal, posterior insular, lateral orbital, parietal, perirhinal, postrhinal, piriform, prelimbic, retrosplenial, primary visual), thalamus (anterior, lateral dorsal, medial dorsal, reuinens nuclei), amygdala (basolateral-lateral, central nuclei), medial septum, mammillary nucleus, and striatum (dorsomedial, medial). A structural ROI was manually drawn on the template brain, as defined by the rat brain atlas. [17] A functional ROI was created by combining anatomically defined ROIs with the significant SPM clusters through logical conjunction as previously described.[7] Mean optical density of each functional ROI was extracted for each animal using the Marsbar toolbox for SPM (version 0.42, http://marsbar.sourceforge.net/). Pearson's correlation coefficients between each pair of ROIs were calculated across subjects within a group in Matlab (version 6.5.1, Mathworks, Inc., Natick, MA, USA) to construct a correlation matrix for each treatment group. Pearson's coefficients (r) were then transformed into Z scores using the Fisher transformation. [29] Correlation matrices were plotted as heatmaps in Matlab. Statistical significance of between-group differences in correlation coefficients was evaluated using the Fisher's Z-transform test ($P < 0.05$).

3. Results

3.1. Behavior

Rats rapidly learned the spatial navigation task within 4–7 days (Fig. 1). Thereafter, they asymptotically improved their latency to find the target, until on day 19, they reached an average time (± standard deviation) of finding the target in 7.8 ± 1.9 seconds from the instant of release. During the brain mapping there were no significant group differences in the time spent exploring the maze prior to triggering of the pump, or in the number of squares traversed on a virtual grid superimposed on the image of the maze (LEARNERS: 18.8 ± 5.2 sec, 17.1 ± 3.7 squares; CONTROLS: 20.1 ± 6.5 sec., 12.8 ± 3.4 squares).

3.2. Statistical Parametric Mapping of the Brain

Significant group differences in rCBF obtained after statistical parametric mapping are shown in the form of significant T-scores mapped onto select coronal sections of the rat brain (Fig. 2). A comprehensive list of significant group differences is shown in Tables 1 and 2. Figure 3 summarizes in graphical form our imaging results within the context of the spatial navigation circuit.

Hippocampal formation and parahippocampus: The pattern of hippocampal activation of LEARNERS compared to CONTROLS differed in dorsal and ventral aspects of the hippocampus (HPC). In the dorsal HPC (septal pole, anterior to bregma −4.0 mm), increases in rCBF were noted bilaterally in a limited area of the dorsal CA1, surrounding the hippocampal fissure. In the ventral HPC, a broader activation was noted in CA1–3 (temporal pole, intermediate and ventral portions) [30], with the most significant changes ($P<0.0005$ for >100 significant contiguous voxels) noted in the distal, ventral CA3 region surrounding the hippocampal fissure and border to CA1 and CA2, and with no significant changes in the dentate gyrus. In addition, significant increased rCBF was noted posteriorly in the ventral subiculum and the posterior subiculum transition area. rCBF also showed small significant increases in both the posterior entorhinal cortex (central, dorsolateral, medial), perirhinal and postrhinal cortices in LEARNERS compared to CONTROLS.

Cerebral cortex: Significantly greater rCBF of LEARNERS compared to CONTROLS was noted in the auditory, cortical amygdaloid, olfactory, orbital (lateral, ventral), parietal (posterior, lateral association), prelimbic, primary and secondary visual cortex, primary somatosensory (barrel field, hindlimb, upper lip), secondary somatosensory, and retrosplenial cortices (dorsal dysgranular region). Significant decreases in rCBF were noted in posterior insular cortex (granular, dysgranular).

Thalamus: Within the thalamus greater rCBF was noted in LEARNERS compared to CONTROLS in the anterior (dorsal/ventral), centrolateral, posterior, lateral posterior, lateral dorsal, habenula, ventral posteromedial, lateral geniculate and medial geniculate nuclei, as well as the combined midline nuclei (reuinens, rhomboid, submedius).

Subcortical motor regions: The striatum showed significantly increased rCBF in LEARNERS compared to CONTROLS in dorsal, dorsomedial, and medial regions, as well

as in the nucleus accumbens shell. Significantly decreased rCBF was noted in the external globus pallidus. Significantly increased rCBF was noted also in the red nucleus. Within the cerebellum, significantly increased rCBF was noted in the first-third cerebellar lobules (vermis), crus1, and the medial vestibular nucleus, with significantly decreased rCBF in the simple lobule.

Limbic and paralimbic regions: Significantly increased rCBF was noted in LEARNERS compared to CONTROLS in the posterior lateral hypothalamus, preoptic area (lateral, magnocellular), medial septal nucleus, caudal linear raphe nucleus, with a significant decrease in rCBF noted in the amygdala (central, basolateral/lateral nuclei, as well as amygdala-piriform transition area) and mammillary nucleus.

Other subcortical regions: LEARNERS compared to CONTROLS showed significantly greater rCBF in the oculomotor nucleus, lateral superior olive, ventral cochlear nucleus, anterior pretectal nucleus, interpeduncular nucleus, endopiriform nucleus, inferior and superior colliculi, and dorsal tegmental nucleus.

Implementation of the false discovery rate (FDR) in SPM revealed seven large clusters that included multiple subregions significant after correction for the FDR at the cluster level ($P < 0.05$). These are shown with asterisks in Tables 1 and 2, and constituted the majority of regions cited above.

3.3 Interregional correlation analysis

LEARNERS, as well as CONTROLS, showed significant positive interregional correlation within subfields of the HPC, including CA1–3 and the dentate gyrus (Fig. 4). Significant positive interregional correlation was also noted between several cortical regions (retrosplenial, lateral orbital, parietal, primary visual and auditory). The aforementioned cortical regions generally showed a positive correlation with the hippocampal regions in LEARNERS, while this correlation was negative in CONTROLS. In addition, the mammillary nucleus and posterior entorhinal cortex showed a positive correlation with the hippocampal regions in CONTROLS, but a negative correlation in LEARNERS.

Fisher's Z-transform test showed in LEARNERS compared to CONTROLS significantly more positive interregional correlation between the HPC (CA1–3) and cerebral cortex (retrosplenial, orbital, parietal and primary visual). A significantly more positive correlation was also noted between the CA3 field and the medial septum. LEARNERS compared to CONTROLS showed significantly more negative interregional correlation between the HPC (CA1–3) and the mammillary nucleus, posterior entorhinal cortex, as well as subregions of the amygdala (central nucleus, basolateral/lateral nucleus←→CA1, basolateral/lateral nucleus←→CA3). A significantly more negative correlation was also noted between the anterior thalamic nucleus and CA2.

4. Discussion

4.1. Functional brain mapping in freely moving animals

Functional activation of the brain during performance of the Morris Water maze and the radial arm maze in rats has been examined using immediate-early gene imaging (e.g. c-fos, zif268) [31–33] and deoxyglucose metabolic mapping.[34–36] These methods, however, have a limited temporal resolution and provide signals that are integrated over 15 minutes or more, during which time a number of other behaviors not directly relevant to learning and memory may be active. Electrophysiologic studies [37] in nonrestrained rodents, while able to deliver excellent temporal resolution, have focused largely on changes in individual brain regions and have not offered a whole brain perspective of functional changes needed to validate the circuitry proposed to underlie spatial navigation. The current method addresses several of the potential restrictions of prior methods through administering radiotracers to conscious, freely moving animals using an implantable minipump and analyzing rCBF from autoradiographic images of the three-dimensionally reconstructed brains. Unique to the current method is its ability to simultaneously provide several features advantageous for functional imaging in small animals: freedom from sedation and immobilization of the animal, acceptable spatial and temporal resolution, and availability of whole brain analysis.

4.2. Multimodal sensory circuits

The Barnes maze task exposed animals to a broad range of sensory inputs. While at the point of brain mapping, both groups were actively exploring the maze, LEARNERS compared to CONTROLS showed greater rCBF in a broad range of sensory pathways, including visual, somatosensory, olfactory, auditory and vestibular circuits. Thus, LEARNERS compared to CONTROLS showed greater functional brain activation in the visual system included the visual cortex, lateral geniculate, anterior pretectal area, superior colliculus, and lateral posterior thalamic nucleus.[38] Greater activation in the somatosensory circuit included the primary somatosensory cortices mapping the whiskers and upper lip, the somatosensory thalamus mapping the whisker fields, face and jaw (ventral posterior medial thalamus, posterior nucleus), anterior pretectal nucleus, zona incerta, and superior colliculus—possibly reflecting greater sensory exploration by LEARNERS of the maze environment.[39] In addition, engagement of olfactory brain regions were greater in LEARNERS than CONTROLS, with greater rCBF noted in the olfactory nucleus, piriform cortex, the cortical amygdala and lateral entorhinal cortex [40]. Greater activation in the auditory circuit [41] included the auditory cortex, medial geniculate, inferior colliculus, lateral superior olive, and ventral cochlear nucleus—suggesting that LEARNERS compared to CONTROLS may have been more attentive to the background white noise present during the time of maze exploration, either making use of sound to help their navigation or because of a possible association of sound with evoked recall.[42] Vestibular cues were also engaged, with increased rCBF noted in LEARNERS in the medial vestibular nucleus, and the first-third cerebellar lobules (part of the cerebellum’s vestibular system), as well as in the thalamus (posterior, medial geniculate, ventrolateral geniculate nuclei), visual, parietal and retrosplenial cortices, medial septum, and dorsal tegmental nucleus – all nodes through which vestibular signals reach the HPC and the entorhinal cortex, and important in the vestibular-ocular reflex.[43] Significant rCBF changes were also noted in LEARNERS in

brain regions that comprise a circuit engaged in defining the animal's head-direction, including the dorsal tegmental nucleus, mammillary nucleus, anterior thalamic nucleus, lateral dorsal thalamic nucleus and retrosplenial cortex.[44]

Our results showed that, not only does spatial navigation involve integration of multimodal sensory inputs, functional brain responses were enhanced in animals that used these inputs to provide information concerning sensory body orientation, reference frame, and movement control. This unexpected finding suggests that learning itself may change neuronal excitability of the multisensory inputs on which the learning depends. In fact, a substantial literature using a variety of functional methods (metabolic mapping, early gene responses, calcium imaging, electrophysiology) documents that associative learning can enhance or diminish functional brain responses to sensory stimuli that otherwise carry no distinct emotional/motivational valence. This phenomenon is well studied in the barrel field cortex, where both functional, molecular and structural changes have been associated with fear conditioned stimulation of the whiskers (reviewed in Siucinska 2017) [45]. Similar observations have been made in the visual pathway [46, 47], olfactory regions [48], vestibular nucleus [49] and auditory cortex [42].

4.3. Spatial navigation circuit

Significant increases in rCBF were noted in LEARNERS compared to CONTROLS broadly across the spatial navigation circuit (Fig. 3), including the HPC (dorsal CA1, ventral CA1–3), subiculum, anterior nucleus of the thalamus, striatum, medial septum, cerebral cortex (visual, auditory, parietal, orbital, prelimbic, retrosplenial posterior entorhinal, piriform, perirhinal, postrhinal), with decreases noted in the mammillary nucleus, amygdala and insula.

Hippocampus: The HPC plays a central role in the retention and retrieval of allocentric spatial memory, though its role may change as acquired information is gradually transformed from a labile to an enduring stable memory (see discussion below).[36] In agreement with prior reports, our study showed that retrieval of spatial memory following acquisition of the Barnes maze task resulted in significant activation across the hippocampus (anterior, dorsal CA1, posterior CA1–3 (ventral, intermediate)) (Fig. 2). The hippocampal formation (hippocampus, subiculum, dentate gyrus) receives the final outputs from all association cortices, and processes and integrates this diverse information.[50] The anterior third of the HPC is functionally distinct from the posterior two-thirds, with the dorsal HPC (septal pole) being dominant during the acquisition of spatial memory, and both dorsal and ventral hippocampi (temporal pole) engaged during retrieval of such a memory.[51, 52]

In our study, LEARNERS demonstrated a broad, significant activation in the ventral hippocampus (ventral, intermediate), with a more circumscribed significant activation in the anterior, dorsal hippocampus. This is consistent with past work that has suggested a prominent role, for ventral HPC during retrieval. Most significant changes were noted in distal, ventral CA3 suggesting a prominent role of CA3 in retrieval.[53–56] There was a relative absence of significant rCBF changes in the dentate gyrus. These results are consistent with the idea previously proposed by others that CA1 and CA3 are critical for

consolidation or retrieval processes, whereas the dentate gyrus is more important in encoding of spatial information, and reduces its influences during late training [31, 53, 57] (but see also [36, 58]). Nevertheless, while the dentate gyrus was clearly spared in the posterior ventral HPC and in anterior medial aspects of the dorsal HPC, the close juxtaposition of the dentate with the CA1 region around the hippocampal fissure in anterior lateral aspects of the dorsal HPC, where activation was noted, made it difficult, given the spatial resolution (100 μm) of our methods, to definitively exclude group differences in that subregion of the anterior dentate gyrus that borders the hippocampal fissure.

Cortex: The bi-directional flow of information between the HPC and neocortex is mediated by the entorhinal, perirhinal and postrhinal cortices.[59, 60] Entorhinal cortex is the principle source of afferents to the HPC. It receives input from the postrhinal and perirhinal cortices in addition to other cortical areas. The perirhinal cortex is thought to be involved in the identification of non-spatial stimuli, while the postrhinal cortex is thought to be more critical for spatial memory.[61] Our study found activation of entorhinal, perirhinal cortex, as well as postrhinal cortex. These findings are consistent with work by Bontempi [35] and others [36], which have shown that during memory consolidation, as acquired information is gradually transformed from a labile to an enduring stable memory, there is increasing recruitment of regions outside the HPC, namely cortical areas.

Our findings showed a robust bilateral activation of dysgranular retrosplenial cortex (RS) in LEARNERS compared to CONTROLS. Previous reports have described head direction and place cells in the RS and damage to the RS results in deficits in spatial navigation. A role for RS has been proposed as an integrator between the HPC and other cortical and subcortical structures. Dysgranular RS has been proposed based on its greater structural connectivity to visual areas and immediate-early gene responses to be particularly important for processing visually guided spatial navigation and memory. [62–64]

Prefrontal, and cingulate cortices are neocortical areas that modulate the retrieval of remote spatial memories.[32, 33, 65, 66] Electrophysiologic recordings have shown a significant proportion of neurons from the prelimbic/infralimbic regions of medial prefrontal cortex display location-specific firing during retrieval of a spatial navigation task, with a greater effect noted for prelimbic/infralimbic cells compared to cells in the anterior cingulate area. [67] Orbital cortex while encoding information related to general motivational significance, also encodes spatiomotor variables needed to evaluate goal-directed decisions.[68] Results of our study are in agreement with these findings. The absence of activation in the anterior cingulate may reflect our short retrieval delay which may have decreased the effort necessary to access previously learned information compared to that inherent for retrieval delays of 30 days (remote memory) for which a role of the anterior cingulate has been reported.[32, 65] Alternatively, differences in environmental conditions (e.g. environmental cues, complexity) may have contributed.[65]

Thalamus: LEARNERS compared to CONTROLS showed increased rCBF in several thalamic nuclei during the recall of spatial memory: the anterior nucleus (dorsal/ventral), lateral dorsal (LD), midline nuclei (reuinens, rhomboid, submedius), habenula, ventromedial (VM) and posterior nuclei (Po). Previous behavioral and physiological studies in the rat have

demonstrated that the anterior thalamic nuclei [69, 70] and lateral dorsal nucleus [71] contain cells which discharge as a function of the direction of the animal's head, such cells are the targets of corticothalamic projections from cells in the retrosplenium [72, 73], and lesions of these regions impair spatial navigation.[74–76] Other nuclei, including the rhomboid and reuinens nuclei [77, 78], and habenula [79], also play a role during recall of a spatial navigation task, with relative sparing of the mediodorsal thalamic nucleus [80]. The posterior nucleus receives somatosensory, auditory, visual and vestibular inputs, with a proposed function of monitoring the motor and sensory dynamics of self-initiated whisker movements.[81] Others have proposed a role of the posterior nucleus in the detection of spatial contrasts.[82] Our results are consistent with these prior findings, providing confirmation using functional brain mapping.

Striatum: Our study showed significant increases in rCBF in LEARNERS compared to CONTROLS dominantly in the medial and dorsomedial striatum an area that has been linked to action-outcome learning including spatial navigation.[83–85] Increases in the dorsal striatum are consistent with prior electrophysiologic recordings that have shown task-responsive phasic neuronal activity during sequential navigation.[37] Small significant increases in rCBF were also noted in the nucleus accumbens, a region proposed to play a role in spatial navigation by integrating information related reward, emotion, as well as context.[86]

Other regions: Our study found significant differences during recall in several additional regions implicated through prior lesion studies as playing a role in the performance of a spatial learning task. These included the medial septum [87], the anterior portions of the cerebellar vermis and cerebellar crus 1 [88, 89], as well as the interpeduncular nucleus--regions proposed to play a role in the integration of vestibular and visual input into the motor output needed to reach a target. Our results substantiate the importance of these cerebral regions in the recall of a spatial navigation task.

4.4. Functional connectivity

Interregional correlational analysis showed that LEARNERS compared to CONTROLS demonstrated significantly altered functional connectivity between regions within the spatial navigation circuit. LEARNERS showed a significantly greater positive correlation of rCBF of the HPC (ventral, posterior CA1–3) with retrosplenial, lateral orbital, parietal and primary visual cortex, as well as a significantly more negative correlation of rCBF of the HPC with posterior entorhinal cortex, the mammillary nucleus, the amgydala (central nucleus, basolateral/lateral nuclei), and the anterior thalamic nucleus (posterior CA2←→ATN). Our functional connectivity results in the Barnes maze underscore the importance of a wider network structure that modulates the hippocampus in the recall of a spatial navigation task. Consistent with this, recent electrophysiologic work in rats has shown that following lesions of the mammillothalamic tract, there is an increase in absolute coherence between the hippocampus and retrosplenial cortex [90], and stimulation of hippocampal output via the descending fornix projections yields a negative correlation between theta power and the field potential observed in electrophysiologic recordings from the anterior thalamic nucleus [91].

Two major pathways carrying afferent and efferent fibers to the hippocampus are the fornix and entorhinal cortex, with additional direct connections of the hippocampus to the amygdala. Connections of the precommissural branch of the fornix include the nuclei of the septum, orbital cortex and anterior cingulate cortex. Connections of the postcommissural branch of the fornix include the mammillary bodies and the anterior nucleus of the thalamus. One may speculate that spatial learning may elicit functional changes within the hippocampus in which activity in neural connections of the postcommissural fornix, as well as activity in the entorhinal cortex, are differentially regulated to functional changes noted in the hippocampal neural connections of the precommissural fornix.

Of note, significant differences in functional connectivity were largely absent between LEARNERS compared to CONTROLS for the dentate gyrus, perirhinal and postrhinal cortex, as well as the striatum (dorsomedial, medial). The lack of significant functional connectivity of the dentate gyrus with remaining regions of the spatial navigation circuit is consistent with prior work suggesting a reduced influence of the dentate gyrus during late stages of training and recall.[31, 53, 57] Our results suggest a continued role for the HPC (CA1–3) in the recall of spatial memories. This underscores that spatial memories after 19 days of training, when performance had reached a stable plateau, may not yet have become independent of the HPC, which may continue to engage in active modulation of cortical regions (retrosplenial, lateral orbital, parietal and primary visual) during spatial recall. While past work suggests that during spatial learning, functional engagement of the HPC may shift along its anterior-posterior extent, the HPC likely continues to play a long-term role despite extensive training.[92]

4.5. Limitations

A number of theories have addressed the neural underpinnings of remote memory, making different predictions regarding hippocampal-neocortical interactions. While there is agreement that the hippocampal complex plays a central role in integrating information processed at the neocortical level during initial stages of spatial learning, the role of the HPC in the retention and retrieval of remote memories is debated, as is the extent of a temporal gradient in the role of the HPC.[93] In brief, Cognitive Map Theory (CMT) posits a central role for the HPC in the retention and retrieval of both recent and remote spatial memories. In contrast, the Standard Consolidation Theory (SCT) predicts that spatial memories become independent of the HPC over time as neocortex and other extrahippocampal structures act to sustain memory traces and their retrieval. Finally, reexamining the literature on which CMT and SCT are based, Multiple Trace theory (MTT) suggests that while remote spatial memories can exist independently of the HPC, this is only the case for schematic or coarse representations of the memory trace (sufficient to support navigation), but not for memories that require recollection of vividness, emotionality and personal significance.[93] In so far as memory rules change from their first association to those that take place when a task is mastered [94], our study did not include examination of the role played by the HPC during early stages of learning, and hence cannot address the issue of changes in the role of the HPC or other structures within the spatial navigation circuit over time.

Several other potential limitations should be considered in the interpretation of our data. While LEARNERS and CONTROLS spent an equivalent amount of time in the maze during the time of brain mapping, their motivations to complete the task may have differed given that the former were trained to seek a reward (escape box), while the latter were simply exposed to the maze. In addition, given that the perfusion tracer was injected at a time when the animal approached the target hole which, however, unlike prior times, had its safe-box removed, we cannot rule out that a component of mismatch of expectation with experience and stress from not being able to escape may have been captured in our brain map. Finally, our functional brain mapping used a threshold for significance ($P < 0.05$ at the voxel level) and used the cluster-extent based thresholding (>100 contiguous significant voxels) commonly used in neuroimaging studies. The minimum cluster criterion was applied to avoid basing our results on significance at a single or small number of suprathreshold voxels, with most clusters containing voxels significant at $P < 0.005$ or $P < 0.0005$ as noted in figure 2. Additional factors suggest the significance of our results. Such effects included the presence of left–right symmetry and the correspondence of clusters within the boundaries of known anatomical structures. These are not statistically captured by the SPM software but increase the confidence of clusters found significant by the SPM algorithm. Given the large number of voxels, one cannot rule out that individual findings may have been due to the multiple comparisons, Nevertheless, our results in most brain regions remained significant after correction for false discovery rate at the cluster level.

4.6. Conclusion

Our study's significance has several aspects: First, our study highlighted that brain mapping facilitated by an implantable minipump represents a novel tool for the whole brain evaluation of complex mammalian behaviors. Second, our functional brain maps underscored the complex sensory component of the experimental spatial navigation task which included broad activation of visual, auditory, somatosensory, olfactory and vestibular brain regions. Interestingly, our results suggest that LEARNERS engage these sensory circuits more actively than CONTROLS. Future work may wish to also include a passive, resting group to explore the somatosensory engagement of controls more fully. Third, our results are consistent with a model established on the basis of prior studies which shows that recall of a spatial navigation strategy after 19 days of learning engages large aspects of ventral HPC and localized aspects of dorsal HPC, with largely a sparing of the dentate gyrus. Finally, our results demonstrated LEARNERS compared to CONTROLS showed increased positive functional connectivity of the ventral HPC to select cortical regions (parietal, visual, orbital, retrosplenial), as well as the medial septum, whereas a negative correlation was noted for the ventral HPC with posterior entorhinal cortex, mamillary nucleus, amygdala, and anterior thalamic nucleus – suggesting differences in modulation by the HPC of these cortical and subcortical regions.

Acknowledgements

We would like to thank Chris Jew and Joseph Tedeschi with their help in the behavioral training, as well as Yumei Guo. This research was supported by the NIBIB (R01 NS050171), the USC/Rose Hills Foundation Student Science and Engineering Research Fellowship, and the USC Medical Student Summer Research Fellowship.

References

[1]. Barnes CA, Memory deficits associated with senescence: a neurophysiological and behavioral study in the rat, J Comp Physiol Psychol 93(1) (1979) 74–104. [PubMed: 221551]

[2]. Gsell W, De Sadeleer C, Marchalant Y, MacKenzie ET, Schumann P, Dauphin F, The use of cerebral blood flow as an index of neuronal activity in functional neuroimaging: experimental and pathophysiological considerations, J Chem Neuroanat 20 (2000) 215–224. [PubMed: 11207420]

[3]. Keri S, Gulyas B, Four facets of a single brain: behaviour, cerebral blood flow/metabolism, neuronal activity and neurotransmitter dynamics, Neuroreport 14(8) (2003) 1097–106. [PubMed: 12821790]

[4]. Holschneider DP, Maarek JM, Harimoto J, Yang J, Scremin OU, An implantable bolus infusion pump for use in freely moving, nontethered rats, Am J Physiol Heart Circ Physiol 283(4) (2002) H1713–9. [PubMed: 12234827]

[5]. Moore WH, Holschneider DP, Givrad TK, Maarek JM, Transcutaneous RF-powered implantable minipump driven by a class-E transmitter, IEEE Trans Biomed Eng 53(8) (2006) 1705–8. [PubMed: 16916107]

[6]. Stumpf WE, Solomon HF, Autoradiography and Correlative Imaging, Academic Press, New York, 1995.

[7]. Wang Z, Pang RD, Hernandez M, Ocampo MA, Holschneider DP, Anxiolytic-like effect of pregabalin on unconditioned fear in the rat: an autoradiographic brain perfusion mapping and functional connectivity study, Neuroimage 59(4) (2012) 4168–88. [PubMed: 22155030]

[8]. Goldman H, Sapirstein LA, Brain blood flow in the conscious and anesthetized rat, Am J Physiol 224(1) (1973) 122–126. [PubMed: 4566847]

[9]. Patlak CS, Blasberg RG, Fenstermacher JD, An evaluation of errors in the determination of blood flow by the indicator fractionation and tissue equilibration (Kety) methods, J Cereb Blood Flow Metab 4 (1984) 47–60. [PubMed: 6363433]

[10]. Sakurada O, Kennedy C, Jehle J, Brown JD, Carbin GL, Sokoloff L, Measurement of local cerebral blood flow with iodo [14C] antipyrine, Am J Physiol 234(1) (1978) H59–66. [PubMed: 623275]

[11]. Jones SC, Korfali E, Marshall SA, Cerebral blood flow with the indicator fractionation of [14C]iodoantipyrine: effect of PaCO2 on cerebral venous appearance time, J Cereb Blood Flow Metab 11 (2) (1991) 236–41. [PubMed: 1900067]

[12]. Van Uitert RL, Levy DE, Regional brain blood flow in the conscious gerbil, Stroke 9 (1978) 67–72. [PubMed: 341424]

[13]. Nguyen PT, Holschneider DP, Maarek JM, Yang J, Mandelkern MA, Statistical parametric mapping applied to an autoradiographic study of cerebral activation during treadmill walking in rats, Neuroimage 23(1) (2004) 252–9. [PubMed: 15325372]

[14]. Friston KJ, Frith CD, Liddle PF, Frackowiak RS, Comparing functional (PET) images: the assessment of significant change, J Cereb Blood Flow Metab 11(4) (1991) 690–699. [PubMed: 2050758]

[15]. Thevenaz P, Ruttimann UE, Unser M, A pyramid approach to subpixel registration based on intensity, IEEE Trans. Image Process 7(1) (1998) 27–41. [PubMed: 18267377]

[16]. Chumbley JR, Friston KJ, False discovery rate revisited: FDR and topological inference using Gaussian random fields, Neuroimage 44(1) (2009) 62–70. [PubMed: 18603449]

[17]. Paxinos G, Watson C, The Rat Brain in Stereotactic Coordinates, 6th ed., Elsevier Academic Press, New York, 2007.

[18]. Kjonigsen LJ, Leergaard TB, Witter MP, Bjaalie JG, Digital atlas of anatomical subdivisions and boundaries of the rat hippocampal region, Frontiers in neuroinformatics 5 (2011) 1–7. [PubMed: 21472085]

[19]. Burwell RD, Borders and cytoarchitecture of the perirhinal and postrhinal cortices in the rat, J Comp Neurol 437(1) (2001) 17–41. [PubMed: 11477594]

[20]. Soncrant TT, Horwitz B, Holloway HW, Rapoport SI, The pattern of functional coupling of brain regions in the awake rat, Brain Res 369(1–2) (1986) 1–11. [PubMed: 3697734]

[21]. Nair HP, Gonzalez-Lima F, Extinction of behavior in infant rats: development of functional coupling between septal, hippocampal, and ventral tegmental regions, J Neurosci 19(19) (1999) 8646–55. [PubMed: 10493765]

[22]. Barrett D, Shumake J, Jones D, Gonzalez-Lima F, Metabolic mapping of mouse brain activity after extinction of a conditioned emotional response, J Neurosci 23(13) (2003) 5740–9. [PubMed: 12843278]

[23]. Wang Z, Bradesi S, Charles JR, Pang RD, Maarek J-MI, Mayer EA, Holschneider DP, Functional Brain Activation during Retrieval of Visceral Pain-Conditioned Passive Avoidance in the Rat, Pain 152(12) (2011) 2746–56. [PubMed: 21944154]

[24]. Shumake J, Conejo-Jimenez N, Gonzalez-Pardo H, Gonzalez-Lima F, Brain differences in newborn rats predisposed to helpless and depressive behavior, Brain Research 1030(2) (2004) 267–76. [PubMed: 15571675]

[25]. Padilla E, Shumake J, Barrett DW, Sheridan EC, Gonzalez-Lima F, Mesolimbic effects of the antidepressant fluoxetine in Holtzman rats, a genetic strain with increased vulnerability to stress, Brain Res 1387 (2011) 71–84. [PubMed: 21376019]

[26]. Fidalgo C, Conejo NM, Gonzalez-Pardo H, Arias JL, Cortico-limbic-striatal contribution after response and reversal learning: a metabolic mapping study, Brain Res 1368 (2011) 143–50. [PubMed: 21036158]

[27]. Schwarz AJ, Gozzi A, Reese T, Heidbreder CA, Bifone A, Pharmacological modulation of functional connectivity: the correlation structure underlying the phMRI response to d-amphetamine modified by selective dopamine D3 receptor antagonist SB277011A, Magn Reson Imaging 25(6) (2007) 811–20. [PubMed: 17442525]

[28]. Liang Z, King J, Zhang N, Uncovering intrinsic connectional architecture of functional networks in awake rat brain, J Neurosci 31(10) (2011) 3776–83. [PubMed: 21389232]

[29]. Fisher RA, On the ‘probable error’ of a coefficient of correlation deduced from a small sample, Metron 1 (1921) 3–32.

[30]. Fanselow MS, Dong HW, Are the dorsal and ventral hippocampus functionally distinct structures?, Neuron 65(1) (2010) 7–19. [PubMed: 20152109]

[31]. Poirier GL, Amin E, Aggleton JP, Qualitatively different hippocampal subfield engagement emerges with mastery of a spatial memory task by rats, J Neurosci 28(5) (2008) 1034–45. [PubMed: 18234882]

[32]. Teixeira CM, Pomedli SR, Maei HR, Kee N, Frankland PW, Involvement of the anterior cingulate cortex in the expression of remote spatial memory, J Neurosci 26(29) (2006) 7555–64. [PubMed: 16855083]

[33]. Jo YS, Park EH, Kim IH, Park SK, Kim H, Kim HT, Choi JS, The medial prefrontal cortex is involved in spatial memory retrieval under partial-cue conditions, J Neurosci 27(49) (2007) 13567–78. [PubMed: 18057214]

[34]. Prins ML, Hovda DA, Mapping cerebral glucose metabolism during spatial learning: interactions of development and traumatic brain injury, J Neurotrauma 18(1) (2001) 31–46. [PubMed: 11200248]

[35]. Bontempi B, Laurent-Demir C, Destrade C, Jaffard R, Time-dependent reorganization of brain circuitry underlying long-term memory storage, Nature 400(6745) (1999) 671–5. [PubMed: 10458162]

[36]. Ros J, Pellerin L, Magara F, Dauguet J, Schenk F, Magistretti PJ, Metabolic activation pattern of distinct hippocampal subregions during spatial learning and memory retrieval, J Cereb Blood Flow Metab 26(4) (2006) 468–77. [PubMed: 16136058]

[37]. Schmitzer-Torbert N, Redish AD, Neuronal activity in the rodent dorsal striatum in sequential navigation: separation of spatial and reward responses on the multiple T task, J Neurophysiol 91(5) (2004) 2259–72. [PubMed: 14736863]

[38]. Toga AW, Collins RC, Metabolic response to optic centers to visual stimuli in the albino rat: anatomical and physiological considerations, J Compar Neurol 199(4) (1981) 443–464.

[39]. Ebner FF, Kaas JH, Somatosensory System, in: Paxinos G (Ed.), The Rat Nervous System, Elsevier, San Diego, CA, 2015, pp. 675–701.

[40]. Imai T, Construction of functional neuronal circuitry in the olfactory bulb, Seminars in cell & developmental biology 35 (2014) 180–8. [PubMed: 25084319]

[41]. Cheung MM, Lau C, Zhou IY, Chan KC, Cheng JS, Zhang JW, Ho LC, Wu EX, BOLD fMRI investigation of the rat auditory pathway and tonotopic organization, Neuroimage 60(2) (2012) 1205–11. [PubMed: 22297205]

[42]. Holschneider DP, Yang J, Sadler TR, Nguyen PT, Givrad TK, Maarek JM, Mapping cerebral blood flow changes during auditory-cued conditioned fear in the nontethered, nonrestrained rat, Neuroimage 29(4) (2006) 1344–58. [PubMed: 16216535]

[43]. Jacob PY, Poucet B, Liberge M, Save E, Sargolini F, Vestibular control of entorhinal cortex activity in spatial navigation, Frontiers in integrative neuroscience 8 (2014) 38. [PubMed: 24926239]

[44]. Taube JS, The head direction signal: origins and sensory-motor integration, Annu Rev Neurosci 30 (2007) 181–207. [PubMed: 17341158]

[45]. Siucinska E, Neurochemical correlates of functional plasticity in the mature cortex of the brain of rodents, Behav Brain Res 331 (2017) 102–114. [PubMed: 28522222]

[46]. Liguz-Lecznar M, Waleszczyk WJ, Zakrzewska R, Skangiel-Kramska J, Kossut M, Associative pairing involving monocular stimulation selectively mobilizes a subclass of GABAergic interneurons in the mouse visual cortex, J Comp Neurol 516(6) (2009) 482–92. [PubMed: 19672986]

[47]. McIntosh AR, Cooper RM, Gonzalez-Lima F, Metabolic activation of the rat visual system by patterned light and footshock, Neurosci Lett 133(2) (1991) 311–4. [PubMed: 1816513]

[48]. Murata K, Kanno M, Ieki N, Mori K, Yamaguchi M, Mapping of Learned Odor-Induced Motivated Behaviors in the Mouse Olfactory Tubercle, J Neurosci 35(29) (2015) 10581–99. [PubMed: 26203152]

[49]. Bruchey AK, Gonzalez-Lima F, Brain activity associated with fear renewal, Eur J Neurosci 24(12) (2006) 3567–77. [PubMed: 17229105]

[50]. Ono T, Nishijo H, Active spatial information processing in the septo-hippocampal system, Hippocampus 9(4) (1999) 458–66. [PubMed: 10495027]

[51]. Moser MB, Moser EI, Distributed encoding and retrieval of spatial memory in the hippocampus, J Neurosci 18(18) (1998) 7535–42. [PubMed: 9736671]

[52]. Loureiro M, Lecourtier L, Engeln M, Lopez J, Cosquer B, Geiger K, Kelche C, Cassel JC, Pereira de Vasconcelos A, The ventral hippocampus is necessary for expressing a spatial memory, Brain Struct Funct 217(1) (2012) 93–106. [PubMed: 21667304]

[53]. Lee I, Kesner RP, Encoding versus retrieval of spatial memory: double dissociation between the dentate gyrus and the perforant path inputs into CA3 in the dorsal hippocampus, Hippocampus 14(1) (2004) 66–76. [PubMed: 15058484]

[54]. Brun VH, Otnass MK, Molden S, Steffenach HA, Witter MP, Moser MB, Moser EI, Place cells and place recognition maintained by direct entorhinal-hippocampal circuitry, Science 296(5576) (2002) 2243–6. [PubMed: 12077421]

[55]. Nakazawa K, Quirk MC, Chitwood RA, Watanabe M, Yeckel MF, Sun LD, Kato A, Carr CA, Johnston D, Wilson MA, Tonegawa S, Requirement for hippocampal CA3 NMDA receptors in associative memory recall, Science 297(5579) (2002) 211–8. [PubMed: 12040087]

[56]. Flasbeck V, Atucha E, Nakamura NH, Yoshida M, Sauvage MM, Spatial information is preferentially processed by the distal part of CA3: implication for memory retrieval, Behav Brain Res 347 (2018) 116–123. [PubMed: 29518437]

[57]. Schlesiger MI, Cressey JC, Boublil B, Koenig J, Melvin NR, Leutgeb JK, Leutgeb S, Hippocampal activation during the recall of remote spatial memories in radial maze tasks, Neurobiol Learn Mem 106 (2013) 324–33. [PubMed: 23742919]

[58]. Gusev PA, Cui C, Alkon DL, Gubin AN, Topography of Arc/Arg3.1 mRNA expression in the dorsal and ventral hippocampus induced by recent and remote spatial memory recall: dissociation of CA3 and CA1 activation, J Neurosci 25(41) (2005) 9384–97. [PubMed: 16221847]

[59]. Aggleton JP, Vann SD, Oswald CJ, Good M, Identifying cortical inputs to the rat hippocampus that subserve allocentric spatial processes: a simple problem with a complex answer, Hippocampus 10(4) (2000) 466–74. [PubMed: 10985286]

[60]. Steffenach HA, Witter M, Moser MB, Moser EI, Spatial memory in the rat requires the dorsolateral band of the entorhinal cortex, Neuron 45(2) (2005) 301–13. [PubMed: 15664181]

[61]. Burwell RD, Amaral DG, Cortical afferents of the perirhinal, postrhinal, and entorhinal cortices of the rat, J Comp Neurol 398(2) (1998) 179–205. [PubMed: 9700566]

[62]. Vann SD, Aggleton JP, Maguire EA, What does the retrosplenial cortex do?, Nat Rev Neurosci 10(11) (2009) 792–802. [PubMed: 19812579]

[63]. Mitchell AS, Czajkowski R, Zhang N, Jeffery K, Nelson AJD, Retrosplenial cortex and its role in spatial cognition, Brain and neuroscience advances 2 (2018) 1–13.

[64]. Pothuizen HH, Davies M, Albasser MM, Aggleton JP, Vann SD, Granular and dysgranular retrosplenial cortices provide qualitatively different contributions to spatial working memory: evidence from immediate-early gene imaging in rats, Eur J Neurosci 30(5) (2009) 877–88. [PubMed: 19712100]

[65]. Lopez J, Herbeaux K, Cosquer B, Engeln M, Muller C, Lazarus C, Kelche C, Bontempi B, Cassel JC, de Vasconcelos AP, Context-dependent modulation of hippocampal and cortical recruitment during remote spatial memory retrieval, Hippocampus 22(4) (2012) 827–41. [PubMed: 21542054]

[66]. Leon WC, Bruno MA, Allard S, Nader K, Cuello AC, Engagement of the PFC in consolidation and recall of recent spatial memory, Learn Mem 17(6) (2010) 297–305. [PubMed: 20508034]

[67]. Hok V, Save E, Lenck-Santini PP, Poucet B, Coding for spatial goals in the prelimbic/infralimbic area of the rat frontal cortex, Proc Natl Acad Sci U S A 102(12) (2005) 4602–7. [PubMed: 15761059]

[68]. Feierstein CE, Quirk MC, Uchida N, Sosulski DL, Mainen ZF, Representation of spatial goals in rat orbitofrontal cortex, Neuron 51(4) (2006) 495–507. [PubMed: 16908414]

[69]. Taube JS, Head direction cells recorded in the anterior thalamic nuclei of freely moving rats, J Neurosci 15(1 Pt 1) (1995) 70–86. [PubMed: 7823153]

[70]. Jankowski MM, Ronnqvist KC, Tsanov M, Vann SD, Wright NF, Erichsen JT, Aggleton JP, O'Mara SM, The anterior thalamus provides a subcortical circuit supporting memory and spatial navigation, Frontiers in systems neuroscience 7 (2013) 45. [PubMed: 24009563]

[71]. Mizumori SJ, Williams JD, Directionally selective mnemonic properties of neurons in the lateral dorsal nucleus of the thalamus of rats, J Neurosci 13(9) (1993) 4015–28. [PubMed: 8366357]

[72]. Shibata H, Organization of projections of rat retrosplenial cortex to the anterior thalamic nuclei, Eur J Neurosci 10(10) (1998) 3210–9. [PubMed: 9786214]

[73]. van Groen T, Wyss JM, Connections of the retrosplenial dysgranular cortex in the rat, J Comp Neurol 315(2) (1992) 200–16. [PubMed: 1545009]

[74]. Aggleton JP, Hunt PR, Nagle S, Neave N, The effects of selective lesions within the anterior thalamic nuclei on spatial memory in the rat, Behav Brain Res 81(1–2) (1996) 189–98. [PubMed: 8950016]

[75]. van Groen T, Kadish I, Wyss JM, The role of the laterodorsal nucleus of the thalamus in spatial learning and memory in the rat, Behav Brain Res 136(2) (2002) 329–37. [PubMed: 12429394]

[76]. Wolff M, Gibb SJ, Cassel JC, Dalrymple-Alford JC, Anterior but not intralaminar thalamic nuclei support allocentric spatial memory, Neurobiol Learn Mem 90(1) (2008) 71–80. [PubMed: 18296080]

[77]. Loureiro M, Cholvin T, Lopez J, Merienne N, Latreche A, Cosquer B, Geiger K, Kelche C, Cassel JC, Pereira de Vasconcelos A, The ventral midline thalamus (reuniens and rhomboid nuclei) contributes to the persistence of spatial memory in rats, J Neurosci 32(29) (2012) 9947–59. [PubMed: 22815509]

[78]. Cholvin T, Hok V, Giorgi L, Chaillan FA, Poucet B, Ventral Midline Thalamus Is Necessary for Hippocampal Place Field Stability and Cell Firing Modulation, J Neurosci 38(1) (2018) 158–172. [PubMed: 29133436]

[79]. Baker PM, Oh SE, Kidder KS, Mizumori SJ, Ongoing behavioral state information signaled in the lateral habenula guides choice flexibility in freely moving rats, Front Behav Neurosci 9 (2015) 295. [PubMed: 26582981]

[80]. Alcaraz F, Naneix F, Desfosses E, Marchand AR, Wolff M, Coutureau E, Dissociable effects of anterior and mediodorsal thalamic lesions on spatial goal-directed behavior, Brain Struct Funct 221(1) (2016) 79–89. [PubMed: 25260555]

[81]. Veinante P, Lavallee P, Deschenes M, Corticothalamic projections from layer 5 of the vibrissal barrel cortex in the rat, J Comp Neurol 424(2) (2000) 197–204. [PubMed: 10906697]

[82]. Legg CR, Turkish S, Spatial contrast sensitivity changes after subcortical visual system lesions in the rat, Behav Brain Res 7(2) (1983) 253–9. [PubMed: 6830654]

[83]. Holahan MR, Taverna FA, Emrich SM, Louis M, Muller RU, Roder JC, McDonald RJ, Impairment in long-term retention but not short-term performance on a water maze reversal task following hippocampal or mediodorsal striatal N-methyl-D-aspartate receptor blockade, Behav Neurosci 119(6) (2005) 1563–71. [PubMed: 16420159]

[84]. McDonald RJ, King AL, Foong N, Rizos Z, Hong NS, Neurotoxic lesions of the medial prefrontal cortex or medial striatum impair multiple-location place learning in the water task: evidence for neural structures with complementary roles in behavioural flexibility, Exp Brain Res 187(3) (2008) 419–27. [PubMed: 18330551]

[85]. Whishaw IQ, Mittleman G, Bunch ST, Dunnett SB, Impairments in the acquisition, retention and selection of spatial navigation strategies after medial caudate-putamen lesions in rats, Behav Brain Res 24(2) (1987) 125–38. [PubMed: 3593524]

[86]. Shibata R, Mulder AB, Trullier O, Wiener SI, Position sensitivity in phasically discharging nucleus accumbens neurons of rats alternating between tasks requiring complementary types of spatial cues, Neuroscience 108(3) (2001) 391–411. [PubMed: 11738254]

[87]. Kelsey JE, Landry BA, Medial septal lesions disrupt spatial mapping ability in rats, Behav Neurosci 102(2) (1988) 289–93. [PubMed: 3365323]

[88]. Joyal CC, Meyer C, Jacquart G, Mahler P, Caston J, Lalonde R, Effects of midline and lateral cerebellar lesions on motor coordination and spatial orientation, Brain Res 739(1–2) (1996) 1–11. [PubMed: 8955918]

[89]. Petrosini L, Leggio MG, Molinari M, The cerebellum in the spatial problem solving: a co-star or a guest star?, Prog Neurobiol 56(2) (1998) 191–210. [PubMed: 9760701]

[90]. Dillingham CM, Milczarek MM, Perry JC, Frost BE, Parker GD, Assaf Y, Sengpiel F, O'Mara SM, Vann SD, Mammillothalamic disconnection alters hippocampo-cortical oscillatory activity and microstructure: Implications for diencephalic amnesia, J Neurosci (2019).

[91]. Tsanov M, Wright N, Vann SD, Erichsen JT, Aggleton JP, O'Mara SM, Hippocampal inputs mediate theta-related plasticity in anterior thalamus, Neuroscience 187 (2011) 52–62. [PubMed: 21459129]

[92]. Clark RE, Broadbent NJ, Squire LR, Impaired remote spatial memory after hippocampal lesions despite extensive training beginning early in life, Hippocampus 15(3) (2005) 340–6. [PubMed: 15744736]

[93]. Moscovitch M, Nadel L, Winocur G, Gilboa A, Rosenbaum RS, The cognitive neuroscience of remote episodic, semantic and spatial memory, Curr Opin Neurobiol 16(2) (2006) 179–90. [PubMed: 16564688]

[94]. Rossato JI, Zinn CG, Furini C, Bevilaqua LR, Medina JH, Cammarota M, Izquierdo I, A link between the hippocampal and the striatal memory systems of the brain, An Acad Bras Cienc 78(3) (2006) 515–23. [PubMed: 16936940]

[95]. Holschneider DP, Maarek JM, Brain maps on the go: functional imaging during motor challenge in animals, Methods 45(4) (2008) 255–61. [PubMed: 18554522]

[96]. Bird CM, Burgess N, The hippocampus and memory: insights from spatial processing, Nat Rev Neurosci 9(3) (2008) 182–94. [PubMed: 18270514]

Highlights

- We report functional brain mapping in the Barnes maze in freely-moving rats
- An implantable minipump allowed bolus administration of a CBF tracer during recall
- Results showed a prominent role, for ventral hippocampus (CA1–3) during retrieval
- CA1–3 functional connectivity increased to select cortical regions during retrieval
- Brain maps highlighted the complex sensory integration of the spatial navigation task

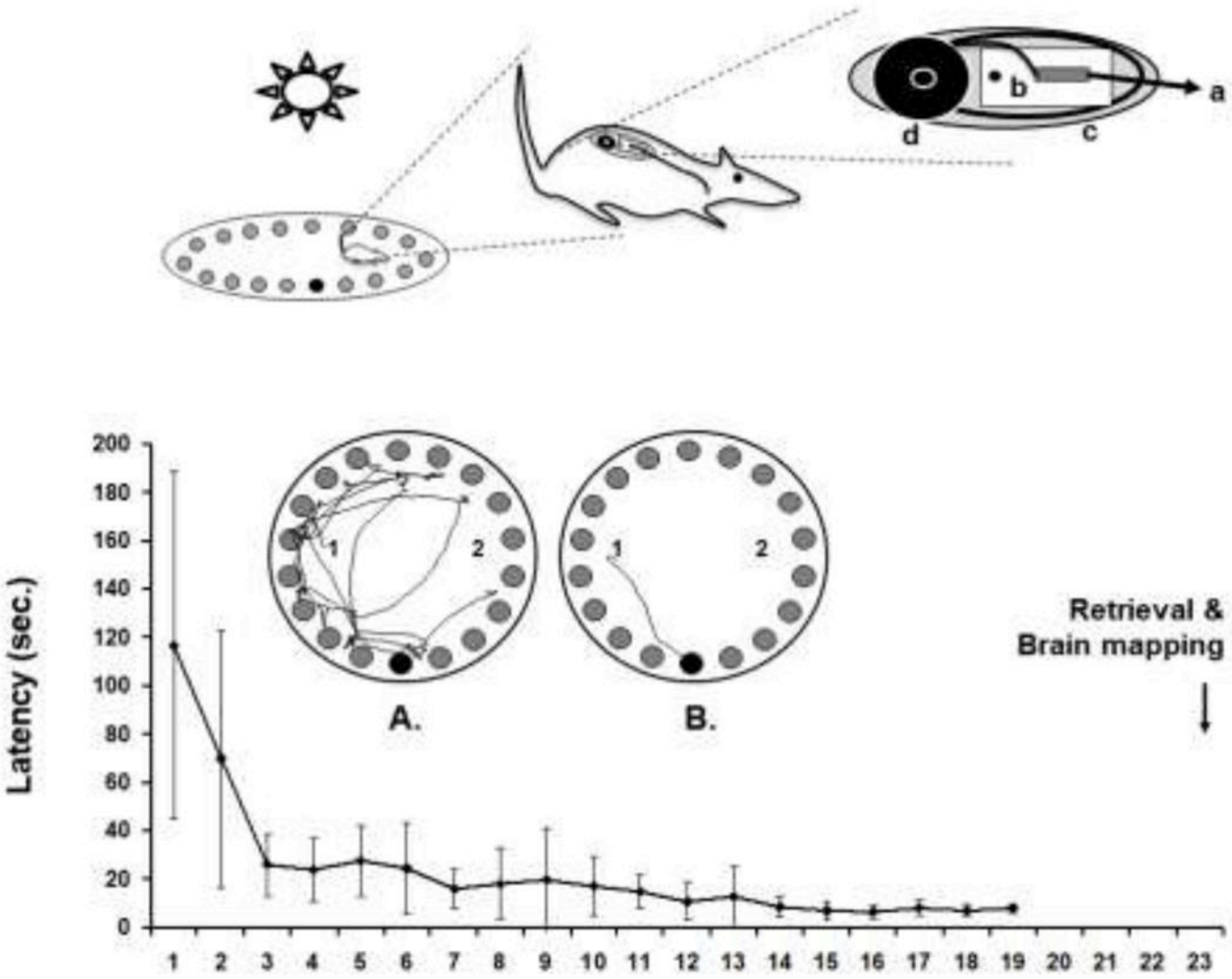

Figure 1: Barnes maze training and delayed recall.

(Top) Rat during performance of the Barnes maze. For the brain mapping, the animal carries a subcutaneously implanted minipump that allows bolus infusion of the cerebral perfusion tracer [^{14}C]-iodoantipyrine by remote-activation using a ceiling mounted infrared light [4, 95]. The pump consists of (a) an intravenous catheter connected to (b) a silicone-embedded solenoid valve powered by a lithium battery rechargeable by wireless power transfer and gated by a frequency-sensitive photodetector, (c) an ejection chamber containing the radiotracer, and (d) a silastic reservoir containing a euthanasia solution. **(Bottom)** Depicted is the group average latency (±SD, n=11) to find the target ‘safe-box’ over 19 days of daily training. The arrow indicates the day of retrieval testing and functional brain mapping. Also shown is a top-down view of the Barnes maze. Rats are released in this example at either the ‘1’ or ‘2’ position, and have to find the ‘escape box’ located below a single one of the available 18 holes (bottom position). The left maze image shows the pathlength of an animal before (A) and after (B) training.

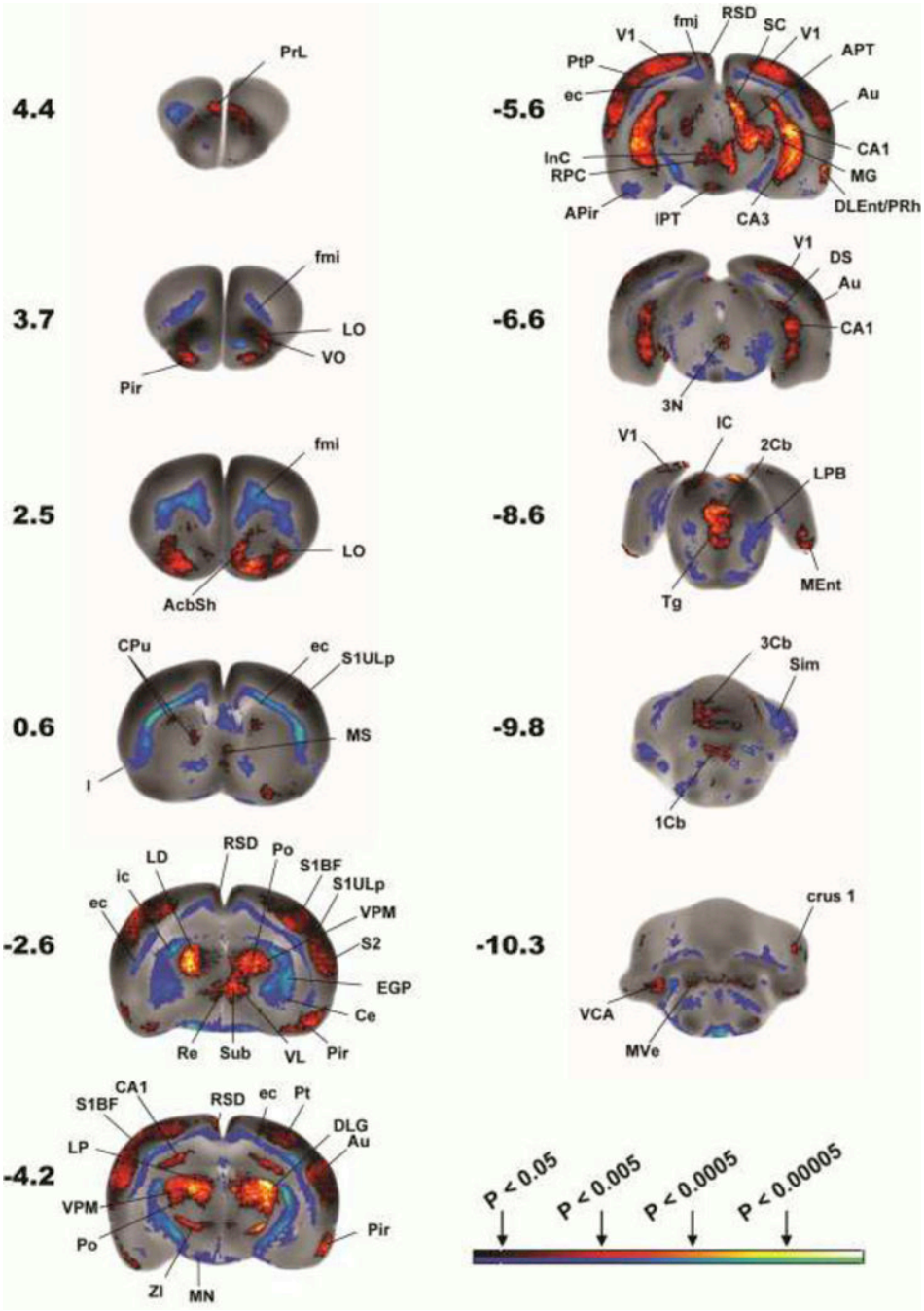

Figure 2. Changes in regional cerebral blood flow related tissue radioactivity in rats during recall.

Comparison is made of functional brain activation between LEARNERS (n=11) and CONTROLS (n=8). Depicted is a selection of representative coronal slices (anterior–posterior coordinates relative to the bregma in millimeters, left side of image represent the right hemisphere). Color-coded overlays show statistically significant positive (red) and negative (blue) differences (P<0.05, >100 significant, contiguous voxels). Regions indicated are according to the Paxinos and Watson rat brain atlas [17] and abbreviations are listed in Tables 1 and 2. The color bar represents p-values (statistical differences) as determined by

the statistical parametric mapping (SPM). The bilateral nature of many of the significant changes, something not accounted for in the SPM analysis, strengthens the significance of the findings.

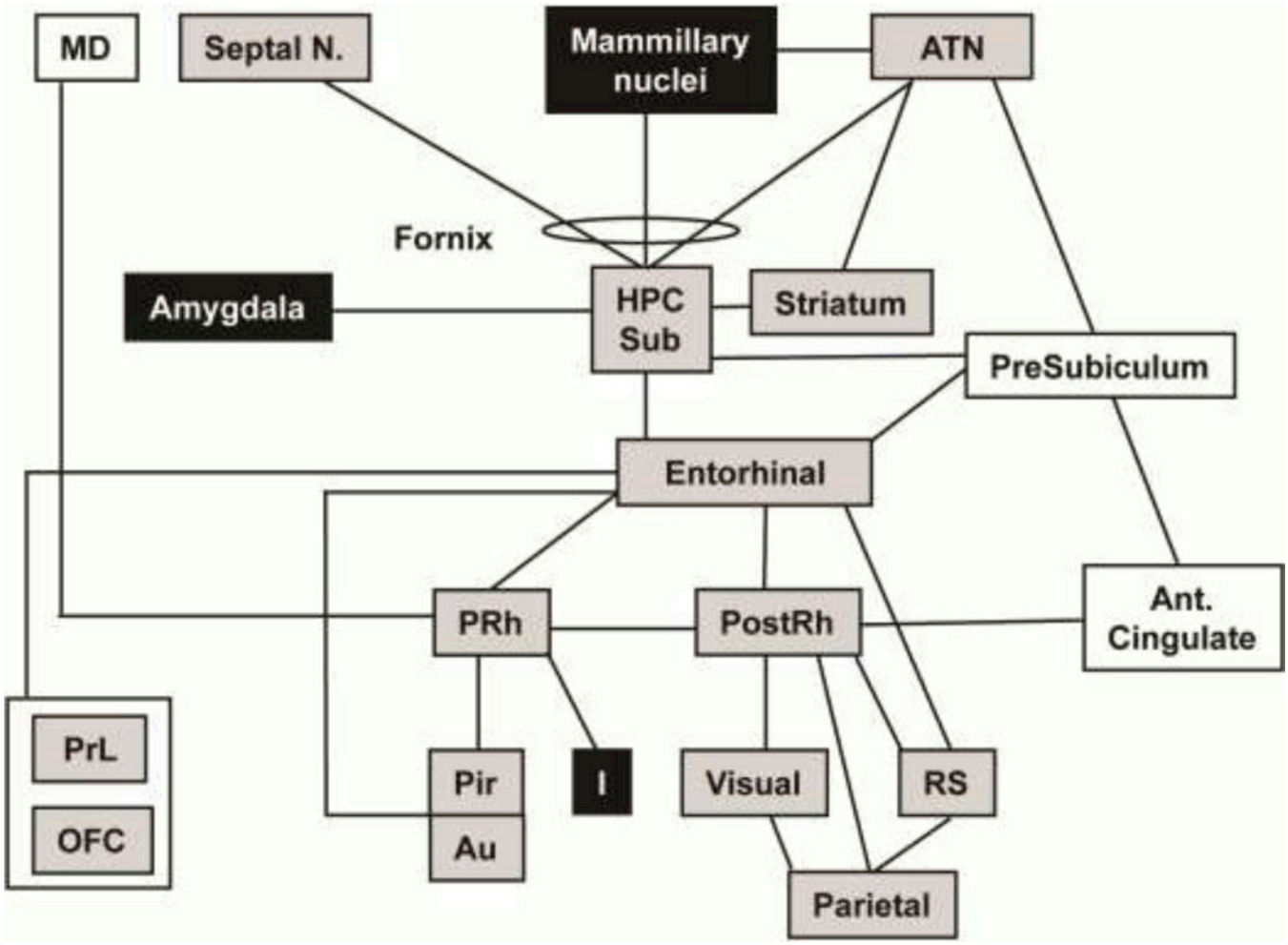

Figure 3. Spatial navigation circuit.

[59, 96] Overlaid onto the circuit are the significant changes in functional brain activation between LEARNERS and CONTROLS during retrieval of spatial memory. Shading indicates a significant increase (gray) or decrease (black) in regional cerebral perfusion ($P<0.05$ for >100 significant, contiguous voxels). No shading indicates no significant change in perfusion. Circuit has been adapted from Bird (2008) and Aggleton (2000), with lines between boxes delineating known major neuronal pathways connecting each region.[59, 96] Abbreviations: ATN (anterior thalamic nucleus), Au (auditory cortex), HPC (hippocampus, posterior CA1–3), I (insular cortex), MD (medial dorsal thalamic n.), OFC (orbitofrontal cortex), Pir (piriform cortex), PostRh (postrhinal cortex), PRh (perirhinal cortex), PrL (prelimbic cortex), RS (retrosplenial cortex), Septal nucleus (medial), Sub (subiculum).

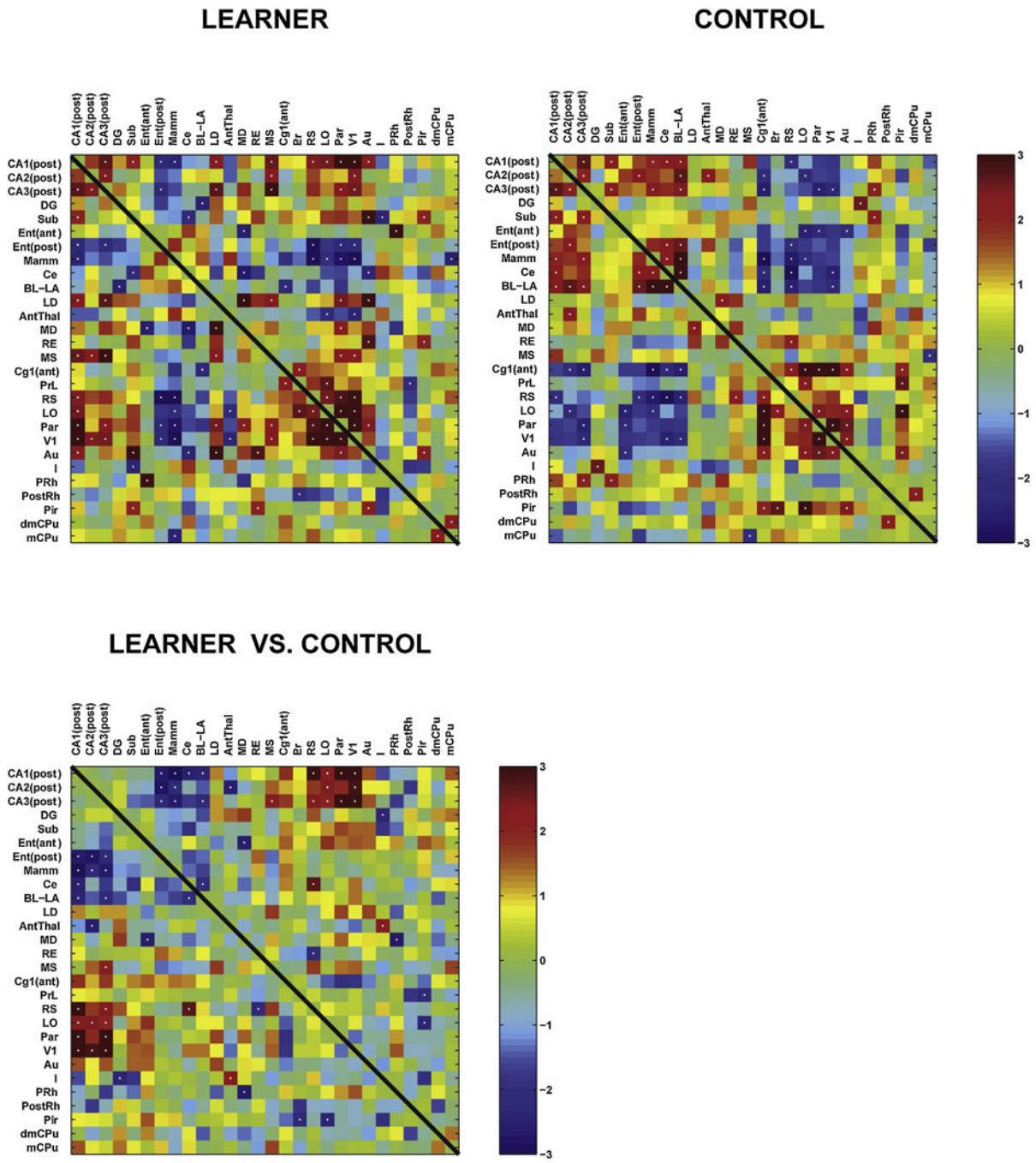

Figure 4: Functional brain connectivity within the extended spatial navigation circuit during active recall of the Barnes maze task.

Interregional correlation matrix shows functional connectivity patterns within the regions outlined in Fig. 3 of LEARNERS and of CONTROLS. Z scores of Pearson's correlation coefficients are color-coded. The matrix is symmetric across the diagonal line from upper left to lower right. Significant correlations ($P<0.05$) are marked with white dots. The bottom matrix of Fisher's Z-statistics represents group differences in Pearson's correlation coefficients (r) between the LEARNERS and CONTROLS. Positive Z values indicate greater r in the LEARNERS group, while negative Z values smaller r. Significant between-

group differences ($P<0.05$) are marked with white dots. Abbreviations as they appear along the figure's axes: CA1 (post) posterior CA1 hippocampal field, CA2 (post) posterior CA2 hippocampal field, CA3 (post) posterior CA3 hippocampal field, DG dentate gyrus, Sub subiculum, Ent (ant) anterior entorhinal cortex, Ent (post) posterior entorhinal cortex, Mamm mammillary nucleus, Ce central nucleus of the amygdala, BL-LA basolateral/lateral amygdaloid nuclei, LD lateral dorsal thalamic nucleus, AntThal anterior thalamic nucleus (dorsal/ventral), LD lateral dorsal thalamic nucleus, RE reuinens nucleus, MS medial septum, Cg1 (ant) anterior, dorsal cingulate cortex, PrL prelimbic cortex, RS retrosplenial cortex, LO lateral orbital cortex, Par parietal cortex, V1 primary visual cortex, Au auditory (temporal) cortex, I insular cortex, PRh perirhinal cortex, PostRh postrhinal cortex, Pir piriform cortex, dmCPu dorsomedial striatum, mCPu medial striatum

Table 1.

Summary of statistically significant differences in cortical functional brain activation during recall.

CORTEX	R/L
Amygdaloid nucleus (cortical): lateral, medial (PLCo, PMCo)	↑/↑
Auditory (Au)	↑/↑ *
Entorhinal (posterior): central, dorsolateral, medial (CEnt, DLEnt, MEnt)	↑/↑ *
Insula (I): posterior granular, posterior dysgranular	↓/↓ *
Olfactory (Tu)	↑/↑ *
Orbital: lateral, ventral (LO, VO),	↑/↑ *
Parietal: posterior, lateral association (Pt, LPtA)	↑/↑ *
Perirhinal (PRh)	/↑ *
Piriform (Pir)	↑/↑ *
Postrhinal (PostRh)	/↑
Prelimbic (PrL, anterior)	↑/↑ *
Retrosplenial, dysgranular (RSD)	↑/↑ *
Somatosensory, primary: barrel field, forelimb, hindlimb, upper lip (S1BF, S1FL, S1HL, S1ULp)	↑/↑ *
Somatosensory, secondary (S2)	↑/↑ *
Visual, primary (V1), secondary (V2)	↑/↑ *

Significant increases (↑) and decreases (↓) are noted for the right and left hemispheres ($P<0.05$ for >100 contiguous significant voxels).

* indicates significant group differences after correction for false discovery rate at the cluster level. Regions are identified as per the Paxinos and Watson rat brain atlas. [14]

Table 2.

Statistically significant differences in subcortical functional brain activation during recall.

SUBCORTEX	R/L
Accumbens nucleus (n.): shell (AcbSh)	↑/↑ *
Amygdala: central n. (Ce), basolateral-lateral n. (BL-LA)	↓/↓ *
Amygdalapiriform transition area (APir)	↓/↓
Caudate Putamen: dorsal, dorsomedial, medial (dCPu, dmCPu, mCPu)	↑/↑ *
Cerebellum: first, second, third lobule (1Cb, 2Cb, 3Cb)	↑ *
crus 1	↑/↑
simple lobule (Sim)	↓/↓
Cochlear n., ventral (VCA)	↑/↑
Colliculus, inferior (IC)	↑/↑
superior (SC)	/↑
Cuneiform n. (Cn)	↓/↓ *
Dorsal tegmental n. (DTg)	↑/↑ *
Endopiriform n. (En)	↑/↑
Globus pallidus, external (EGP)	↓/↓ *
Hippocampus: anterior CA2/CA3, posterior CA1, CA2, CA3	↑/↑ *
Hypothalamus: posterior lateral (PLH)	↑/↑
Interpeduncular n. (IPT)	↑
Mammillary n., (MN)	↓/↓ *
Medial septum (MS)	↑
Oculomotor n. (3N)/Interstitial n. of Cajal (InC)	↑
Parabrachial n. lateral, (LPB)	↓/↓ *
Preoptic area: lateral (LPO), magnocellular (MCPO)	↑/↑
Pretectal area, anterior (APT)	↑/↑ *
Raphe, caudal linear n. (CLi)	↑ *
Red n. (RN)	↑/↑ *
Subiculum: ventral (VS), posterior transition area (STr)	↑/↑ *
Superior olive: lateral (LSO)	↑/↑
Thalamus, anterior (dorsal/ventral, AD/AV)	↑/↑ *-AV
geniculate: dorsolateral, medial, (DLG, MG)	↑/↑ *
habenula (Hb)	↑/↑ *
lateral dorsal, lateral posterior (LD, LP)	↑/↑ *
centrolateral (CL)	↑/↑ *
posterior (Po)	↑/↑ *

SUBCORTEX	**R/L**
submedius (Sub)	↑/↑ *
ventral midline n. (reuinens, rhomboid, submedius)	↑ *
ventral anterior (VA), ventrolateral (VL), ventromedial (VM)	↑/↑ *
ventral posteromedial (VPM)	↑/↑ *
Ventral pallidum (VP)	↓/↓
Vestibular n., medial (MVe)	↑/↑
Zona Incerta (ZI)	↑/↑ *

Significant increases (↑) and decreases (↓) are noted for the right and left hemispheres (P<0.05 for >100 contiguous significant voxels).

* indicates significant group differences after correction for false discovery rate at the cluster level. Regions are identified as per the Paxinos and Watson rat brain atlas. [14]